



HAL
open science

Design of a piping inspection robot by optimization approach

Swaminath Venkateswaran, Damien Chablat, Pol Hamon

► **To cite this version:**

Swaminath Venkateswaran, Damien Chablat, Pol Hamon. Design of a piping inspection robot by optimization approach. The ASME 2020 International Design Engineering Technical Conferences & Computers and Information in Engineering Conference, IDETC/CIE 2020, Aug 2020, Saint-Louis, Missouri, United States. hal-02626029v1

HAL Id: hal-02626029

<https://hal.science/hal-02626029v1>

Submitted on 26 May 2020 (v1), last revised 3 Jun 2020 (v2)

HAL is a multi-disciplinary open access archive for the deposit and dissemination of scientific research documents, whether they are published or not. The documents may come from teaching and research institutions in France or abroad, or from public or private research centers.

L'archive ouverte pluridisciplinaire **HAL**, est destinée au dépôt et à la diffusion de documents scientifiques de niveau recherche, publiés ou non, émanant des établissements d'enseignement et de recherche français ou étrangers, des laboratoires publics ou privés.

DESIGN OF A PIPING INSPECTION ROBOT BY OPTIMIZATION APPROACH

Swaminath Venkateswaran^{1,2}, Damien Chablat^{2,3*}, Pol Hamon²

¹Ecole Centrale de Nantes, Nantes, 44321 France

²Laboratoire des Sciences du Numérique de Nantes (LS2N), UMR CNRS 6004, Nantes, 44300, France

³Centre National de la Recherche Scientifique (CNRS), Nantes, 44321, France

Emails: {swaminath.venkateswaran, damien.chablat, pol.hamon}@ls2n.fr

ABSTRACT

This article presents an optimization approach for the design of an inspection robot that can move inside variable diameter pipelines having bends and junctions. The inspection robot uses a mechanical design that mimics the locomotion of a caterpillar. The existing prototype developed at LS2N, France is a rigid model that makes it feasible for working only inside straight pipelines. By the addition of a tensegrity mechanism between motor units, the robot is made reconfigurable. However, the motor units used in the prototype are oversized to pass through pipe bends or junctions. An optimization approach is employed to determine the dimensions of motors and their associated leg mechanisms that can overcome such bends. Two optimization problems are defined and solved in this article. The first problem deals with the determination of motor sizing without leg mechanisms. The second problem deals with the determination of sizing of the leg mechanism with respect to the dimensions of motor units obtained from the first problem. A 3D model of the optimized robot design is then realized using CAD software.

INTRODUCTION

Manual intervention of pipelines in industries such as nuclear or chemical is cumbersome and risky as it may lead to loss of human life or causes long term radiation effects. Inspection robots play a vital role in such situations as they not only reduce human effort but also can perform a given task with better accuracy. In-pipe inspection robots can be classified [1] viz: Pig

type [2], Wheel type [3], Caterpillar type [4], Wall-press type [5], Walking type [6], Inchworm type [7] and Screw type [8]. A bio-inspired piping inspection robot was designed and developed at LS2N, France [9]. This robot accomplishes the locomotion of a caterpillar in six-steps to move inside a pipeline. Using a slot-follower leg mechanism, the robot attains static postures to establish contact with pipeline walls. The leg mechanisms are capable of working between 40–94 mm diameter straight pipelines [10]. However, the robot is a rigid model and is thus limited to straight pipelines. Also, the spindle drive used in the prototype allows the robot to move at a very low speed of 0.43 mm/s [11]. By the addition of a tensegrity mechanism between the motor modules, the robot is made reconfigurable [12]. The dimensions of the existing motor units are oversized and might restrict the reconfigurable robot to pass through pipe bends at 90°. In this article, an optimization approach is followed to determine the motor sizing that will be capable of overcoming pipe bends. Optimization algorithms can be classified into deterministic and heuristic approaches [13]. The deterministic optimization approach solves problems in a structured manner that leads to efficient solutions with respect to design variables and constraints. On the other hand, heuristic/evolutionary algorithms operate on randomness. Based on the complexity of the design problem, the heuristic approach requires lesser computational times over the deterministic approach [14]. However, there are possibilities that both the algorithms can lead to solutions trapped in a local minimum. For the bio-inspired robot under study, a deterministic approach using *fmincon* is carried out in MATLAB. The problem is solved for a planar test bench where the robot is constructed as multi-

*Address all correspondence to this author

body blocks. Two optimization problems have been solved for determining the optimal robot assembly. The first problem deals with the determination of motor sizes of each module without the presence of leg mechanisms. From the results of optimization, the motors and gear units are identified with catalog products of Maxon based on dimensions, velocity and force factors. The second optimization problem deals with the determination of the geometry of slot-follower leg mechanism that can be accommodated for the motor sizing determined from the results of the first problem. With the geometry of leg mechanisms determined, the working diameter range for the robot under study can be estimated. A 3D model of the optimized robot design is realized using CATIA software.

The outline of the article is as follows. In the following section, the architecture of the robot is presented. The next section deals with the overall problem definition of the optimization process, the representation of the test bench and modeling of robot using MATLAB. The subsequent section deals with the first optimization problem methodology and results. Followed by that the second optimization problem is defined and solved. The article then ends with conclusions.

ARCHITECTURE OF THE ROBOT

The bio-inspired robot developed at LS2N, France comprises of three motor modules which ensure clamping and elongation phases for accomplishing the locomotion of a caterpillar. The motor modules consist of DC brushless motor coupled with a spindle drive to convert rotary motion to prismatic movement [9, 10]. The front and rear modules have 3 sets of slot-follower leg mechanisms each to have contact with the inner walls of pipelines at all instances of locomotion. Through study of design issues namely passive compliance, active compliance and tilt limits [12], a tensegrity mechanism was proposed to be introduced to the robot in order to make it reconfigurable. The tensegrity mechanism comprises of a passive universal joint and three tensions springs. While passing through pipe bends at 90° , the mechanism operates in a passive mode to overcome the bend. In the event of a junction or T-union inside the pipeline, cables that pass through springs of the mechanism can be actuated through external motors for tilting the tensegrity mechanism along a given direction. By workspace analysis with respect to joint limits of springs, an inverse pendulum configuration is employed for the tensegrity mechanism [15]. A 3D model of the bio-inspired robot with the tensegrity mechanism is represented in Fig. 1. In Fig. 1, T_1 and T_2 represent the tensegrity mechanisms. The CAD model depicted in Fig. 1 is constructed using the motors employed in the rigid prototype. If this reconfigurable robot is employed within a pipeline having diameters less than 100 mm, the modules can get trapped in the bends or elbows as the dimensions of the motor units prove to be oversized. For determining the dimensions of motors and leg mechanisms that can

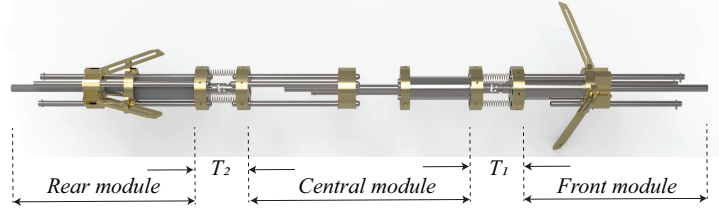


FIGURE 1: 3D model of the existing bio-inspired robot with the tensegrity mechanisms

overcome such bends, an optimization approach is being implemented.

PROBLEM DEFINITION

In this article, two optimization problems are solved to determine the robot assembly. The first problem deals with the determination of motor sizes of each module without the presence of leg mechanisms. To simplify the computation, the dimensions of the tensegrity mechanism are considered fixed. The optimization problem is tested for pipeline diameters ranging from 70 to 160 mm. Based on the results of optimization, suitable motor units are chosen for the robot from the catalog of Maxon. The second problem is carried out for the results of optimization of the first problem for determining the size of the slot-follower leg mechanism.

Test bench

The optimization problems are solved in a planar test bench. The test bench consists of a horizontal pipe section, a 90° elbow and a vertical pipe section. The optimal sizing is determined especially at the bend section wherein collision of modules against the walls of the pipelines is verified. The test bench for the optimization problem is represented in Fig. 2. The test pipe represented in Fig. 2a is generally manufactured by Numerical Control (NC) bending processes using a roller with its origin at \mathbf{o} and flexible mandrels [16]. The coordinate of point \mathbf{o} is given by $[1.5d, 1.5d]$ where d is the diameter of the pipe. With respect to \mathbf{o} , the trajectories of the test bench are classified as the inner portion, center line radius (CLR) and the outer portion. The bending radius of these trajectories represented in Fig. 2b is given by $[r_1, r_2, r_3] = [d, 1.5d, 2d]$. The optimization problem is solved for a fixed diameter value at any instant. The values considered for d are [70, 80, 90, 100, 110, 120, 130, 140, 150, 160] mm. The pipeline geometry is constructed in MATLAB by sub-dividing into straight and bent cross-sections. The coordinate system for the test bench with respect to \mathbf{o} for Fig. 2a is given in Table 1. A discretization is done between each coordinate wherein the continuous trajectory is being subdivided into discrete counterparts. This discretization is being applied to the walls of the pipelines as

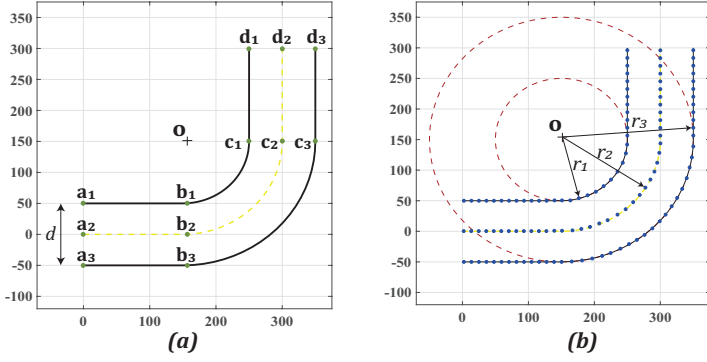


FIGURE 2: Overview of (a) the test bench for optimization and (b) parametrization of the test bench

TABLE 1: COORDINATE SYSTEM OF PIPE GEOMETRY

Coordinate	Inner($i=1$)	Center($i=2$)	Outer($i=3$)
\mathbf{a}_i	$r_1[0,0]$	$r_2[0,0]$	$r_3[0,0]$
\mathbf{b}_i	$r_1[1,0]$	$r_2[1,0]$	$r_3[1,0]$
\mathbf{c}_i	$r_1[2,1]$	$r_2[2,1]$	$r_3[2,1]$
\mathbf{d}_i	$r_1[2,2]$	$r_2[2,2]$	$r_3[2,2]$

well as the CLR and they are represented by blue dotted lines in Fig. 2b. The inner and outer portion discretization is employed to check for collision against modules during locomotion. The discretization of the CLR is mainly used to move the robot and also to rotate the modules. The discretization equations for the straight sections are given by

$$\mathbf{m} = \mathbf{a}_i + n(\mathbf{b}_i - \mathbf{a}_i) \quad (1)$$

$$\mathbf{m} = \mathbf{c}_i + n(\mathbf{d}_i - \mathbf{c}_i) \quad (2)$$

where $n = 0 : 0.01 : 1$ and $i = 1, 2, 3$

In Eqn. (1) & Eqn. (2), \mathbf{m} indicates the coordinates of a discretized point between the start and end points of the straight sections. The bend section of pipe with the discretized points between \mathbf{b}_i - \mathbf{c}_i is constructed using the equation

$$\mathbf{m}_j = \left[r_i \sin\left(\frac{j\pi}{40}\right), -r_i \cos\left(\frac{j\pi}{40}\right) \right] \quad (3)$$

where $j = 0$ to 20 and $i = 1, 2, 3$

Modeling of robot and design variables

The robot is modeled as multi-body planar blocks with a tensegrity mechanism between each module. The motor unit is considered as a combination of brushless DC-motor coupled with a spindle drive. The robot geometry considered for optimization is represented in Fig. 3, where the motor units are represented by rectangular blocks with screw units. The reference frame of the robot Σ_0 is fixed at the center of gravity (CG) position of the central motor unit. The movement of the robot is simulated in MATLAB by displacing the CG of the reference frame to each discretized point on the CLR. For any position of the robot on a given discretized point on the CLR, the rotation angle is applied to the other modules as well as to the tensegrity mechanisms to accomplish the rotation while passing through pipe bends. The rotation of modules during locomotion inside the test bench is accomplished as described below in Algorithm 1.

Algorithm 1 Movement of robot inside the test bench

Inputs: Discretized CLR coordinates, Robot design parameters

Outputs: Rotation angles of modules ($\theta_0, \theta_1, \theta_2$)

- 1: *Initialization*
- 2: **for** $i = 1 - n$ **do** $\triangleright n$ indicates the end point of CLR
- 3: Placing reference frame Σ_0 at starting point of CLR
- 4: Extract the coordinates (x & y) of CLR point coinciding with frame Σ_0
- 5: Apply rotation angle θ_0 to Module-2 by $\theta_0 = \text{atan}\left(\frac{y}{x}\right)$
- 6: Extract the coordinates of CLR point closer to frame Σ_1 .
- 7: Calculate rotation angle θ_1 from the coordinates of point extracted in Step-6
- 8: Apply rotation angle θ_1 to tensegrity mechanism coupled between Module-1 and 2.
- 9: Extract the coordinates of CLR point closer to frame Σ_2 .
- 10: Calculate rotation angle θ_2 from the coordinates of point extracted in Step-9
- 11: Apply rotation angle θ_2 to tensegrity mechanism coupled between Module-2 and 3.
- 12: **end for**

The design variables for the motor unit are given by $[l_{k1}, w_{k1}]$. The screw unit of the spindle drive is defined by $[l_{k2}, w_{k2}]$. Here k indicates a module and it assumes values from 1 to 3. These design parameters are also represented in Fig. 3 for each module. The dimensions of the tensegrity mechanism are fixed and are defined by $[2r_f, 2r_f]$. An inverse pendulum configuration with a value of 11 mm for r_f is chosen [15].

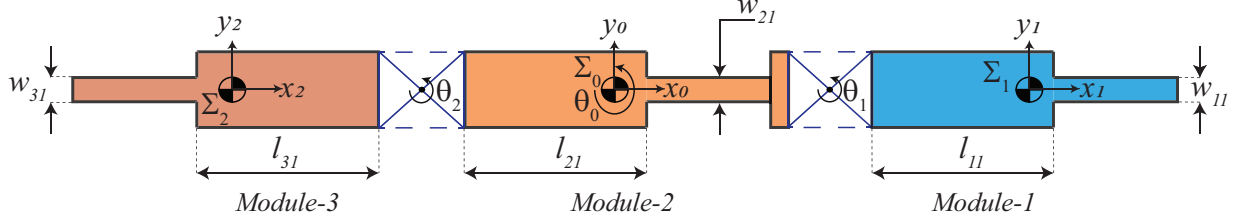


FIGURE 3: Representation of the robot assembly with various design parameters for the optimization problem

FIRST OPTIMIZATION PROBLEM: MOTOR SIZING

A single objective optimization problem subject to constraints is solved using MATLAB. The leg mechanisms are not taken into account for the first optimization problem and an optimal motor sizing is determined at all discretized positions of CLR by avoiding collisions against pipeline walls. As the central module takes care of elongation and retraction phases, it is assumed for the computation that this module remains in fully extended phase at all instances of simulation.

Objective function

The objective function of the problem aims at maximizing the area of the motor units. Since the dimensions of the tensegrity mechanism are fixed, their areas are not taken into account. The area of the robot at a given position of CLR is given by

$$f_1 = \sum_{k=1}^3 (l_{k1}w_{k1} + l_{k2}w_{k2}) \quad (4)$$

where k indicates the module

The area of motor units is estimated as per Eqn. (4). The global sum of f_1 from Eqn. (4) is calculated throughout the discretized points of the CLR and it will be maximized.

Constraint function

For each position of the robot on the CLR, the collision of modules is checked against pipeline walls. Inequality constraints are defined in the optimization problem which will ensure that the modules avoid collision during movement inside the test bench, especially at the bends. A complete discretization of each module is performed. The discretization equation is similar to Eqn. (1) & Eqn. (2). The discretized robot modules inside the test bench is represented in Fig. 4. For each position of reference frame Σ_0 on the discretized CLR trajectory, the points closer and farther on each module from the point \mathbf{o} are extracted. These points can be extracted using the *min* and *max* function of MATLAB. The representation of the points closer (\mathbf{s}_k) and farther (\mathbf{q}_k)

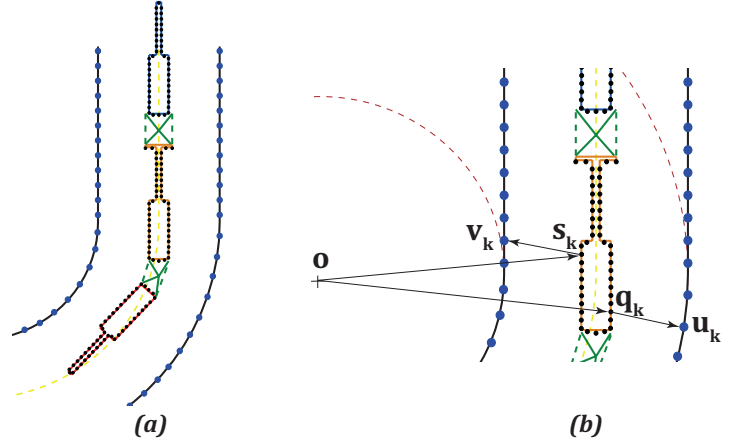


FIGURE 4: (a) Discretized robot assembly and (b) extraction of coordinates from the discretized model for defining constraints

from point \mathbf{o} on a module is shown in Fig. 4b. Followed by that, the point \mathbf{v}_k on the inner portion closer to \mathbf{s}_k and the point \mathbf{u}_k on the outer portion closer to \mathbf{q}_k are extracted using the *min* function. With the extracted set of points, the inequality constraints are defined in MATLAB which ensures that there exist no collisions between modules and pipeline walls. The constraint equations at a given point on CLR are thus defined by

$$g_k : \|\mathbf{oq}_k\| \leq \|\mathbf{ou}_k\| \quad (5)$$

$$g_{k+1} : \|\mathbf{os}_k\| \geq \|\mathbf{ov}_k\| \quad (6)$$

where $k = 1, 2, 3$

Throughout the locomotion sequence, the collisions of modules are checked using Eqn. (5) & Eqn. (6). The pseudo-code for the constraint function and its working in MATLAB is provided in Algorithm 2.

Algorithm 2 Definition of constraint equations in MATLAB

Inputs: Discretized CLR coordinates, Robot design parameters

Outputs: Inequality constraint equations ($g_1, g_2, g_3, g_4, g_5, g_6$)

```

1: Initialization
2: for  $i = 1 - n$  do  $\triangleright n$  indicates the end point of CLR
3:   for  $j = 0 : 0.01 : 1$  do  $\triangleright$  Discretization
4:     Discretize each face of each module
5:   end for
6:   Extract the point ( $s_{ik}$ ) on module  $k$  closer to  $\mathbf{o}$  using  $\min$ 
7:   Extract the point ( $q_{ik}$ ) on module  $k$  farther to  $\mathbf{o}$  using  $\min$ 
8:   for  $l = 1 - n$  do  $\triangleright$  For each discretized point on inner &
outer portions
9:     Calculate  $\|\mathbf{u}_l \mathbf{q}_{ik}\|$ 
10:    Calculate  $\|\mathbf{v}_l \mathbf{s}_{ik}\|$ 
11:  end for
12:  Extract discretized point  $\mathbf{u}_{ik}$  on outer portion closer to  $\mathbf{q}_{ik}$ 
13:  Extract discretized point  $\mathbf{v}_{ik}$  on inner portion closer to  $\mathbf{s}_{ik}$ 
14:  Check inequality constraints ( $g_1, g_2, g_3$ ):  $\|\mathbf{o} \mathbf{q}_{ik}\| \leq \|\mathbf{o} \mathbf{u}_{ik}\|$ 
15:  Check inequality constraints ( $g_4, g_5, g_6$ ):  $\|\mathbf{o} \mathbf{s}_{ik}\| \geq \|\mathbf{o} \mathbf{v}_{ik}\|$ 
16: end for
  
```

Problem statement

With the objective function and constraint function being defined, the first optimization problem can be stated as

$$\text{maximize } \sum_{i=1}^n f_1(\mathbf{x})$$

subject to constraints: $g_1, g_2, g_3, g_4, g_5, g_6$

$$\text{where } \mathbf{x} = [l_1, w_1, l_2, w_2]^T,$$

$i = 1..n$ indicates the discretized CLR points

Since identical motor unit is being employed in each module, only 4 design variables are set instead of 12. The objective and constraint functions are solved using the *fmincon* function in MATLAB. The design variables are subject to lower and upper bounds to have a closer interpretation of the catalog parts of Maxon. The existing prototype uses a brushless DC-motor of diameter 16 mm coupled with a spindle drive GP 16 S. The overall length of this assembly is 58 mm with a screw length of 102 mm. The advantage of using brushless motors is that they offer hall sensors which can be useful in the control phase of the robot to determine pipeline diameters inside unknown/closed environment [17]. The catalog parts of Maxon offers hall sensors for motor diameters starting from 16 mm. The lower (*lb*) and upper bounds (*ub*) for the design variables of the optimization problem are set as $lb = [40, 8, 20, 2]$ and $ub = [60, 16, 102, 5]$. The *lb* of l_1 and w_1 are fixed at 40 mm and 8 mm as this is the minimum size of motor units offered by Maxon [18]. The *ub* of l_1 and w_1 are taken as 60 mm and 16 mm to correlate with the DC-Motor unit

length and diameter of the existing prototype. The *ub* of screw length l_2 is fixed as 102 mm as this is the maximum size offered by Maxon [18]. The *ub* of screw diameter w_2 is set as 5 mm as per the catalog of Maxon. The optimization algorithm is executed with a constant value of diameter throughout the section depicted in Fig. 2a. The algorithm will be evaluated one after the other for pipe diameters from 70 to 160 mm. For faster convergence of the problem and also to satisfy bounds at all iterations, the Sequential Quadratic Programming (SQP) algorithm [19] is employed. The tolerance value for the guess variables and the objective function is set at 10^{-9} .

Results and discussions

As the definition of objective and constraint functions does not have complex parameters, faster convergence is obtained. The dimensions of motor units obtained from the optimization algorithm for the various pipe diameters are provided below in Table 2.

TABLE 2: RESULTS OF OPTIMIZATION PROBLEM-1: SIZING OF MOTOR UNIT

Pipe diameter	l_1	w_1	l_2	w_2
d (mm)	(mm)	(mm)	(mm)	(mm)
70	41.4	12.7	20	2
80	47.44	14	24.7	2
90	50.95	16	32	3.9
100	52.72	16	45.17	5
110	55.02	16	58.25	5
120	58.21	16	71.33	5
130	60	16	84.4	5
140	60	16	86.54	5
150	60	16	98.8	5
160	60	16	102	5

From the results of the optimization provided in Table 2, a gradual increase in all design parameters could be observed. For the 70–80 mm diameter pipe range, a motor width less than 16 mm is observed. Also, the screw diameter for 70–90 mm pipe diameter is found to be less than 5 mm. Thus, the results of optimization for 70–90 mm diameter pipelines have no significance in motor selection from the catalog. Also, it has to be

noted that the screw length l_2 for these pipe diameters is comparatively smaller which might pose an issue when accommodating the slot-follower leg mechanism. Based on the results of Table 2, catalog parts of Maxon are identified for 100 to 160 mm diameter pipelines and they are provided in Table 3. The EC-motor series 283828 of Maxon [18] is chosen for all the combinations. This EC-motor is also being used in the existing prototype. With this motor, three possible spindle drives can be used and will be feasible for 100–160 mm diameter pipelines having bends. The 424731 spindle drive offers the highest velocity. However, the feed force offered by this series is low and might pose a problem during static phases when the leg mechanisms are coupled. The 424744 and 424749 series, on the other hand, have better feed forces. The latter is the spindle drive used in the existing prototype. The disadvantage of this series is that it has a very low output velocity. The total length (l_1) for this spindle drive proves to be oversized for 100 to 120 mm diameter pipes. Taking into account the length, efficiency and velocity factors, the 283282 EC-motor coupled with 424744 spindle drive is chosen for further analysis. From Table 2, it is interesting to note that with the increase in diameter of the pipeline, the screw length l_2 increases. With an 85 mm screw length, it could be possible to accommodate a leg mechanism that can work between 130–160 mm pipelines. However, with this screw length, it might not be possible to work with 100–120 mm pipeline diameters as there might be collisions when passing through bends. In order to have a working model inside smaller diameter pipelines, the optimization results of 100 mm is considered for further analysis with which it would be possible to work inside pipe bends having diameter range between 100 to 120 mm.

SECOND OPTIMIZATION PROBLEM: DESIGN OF SLOT-FOLLOWER LEG MECHANISM

With the optimal motor sizing determined from problem-1, the next step is to determine the geometry of leg mechanisms that could be accommodated within the screw length. The ratio of screw length to the pipe diameter has a greater influence on the geometry of leg mechanisms. The geometry of the slot-follower leg mechanism and its assembly on the existing robot are represented in Fig. 5. By using the inverse kinematic model, the dimensions for the leg mechanism was identified in [10] by a multi-objective optimization approach. In this article, a simple mono objective optimization problem is solved where the dimensions of leg mechanisms are determined through a geometrical approach.

Modeling of the leg mechanisms and design variables

The leg mechanism assembly consists of three legs assembled at 120° with respect to each other [9]. During locomotion, the orientation of leg mechanisms about the axis of robot is un-

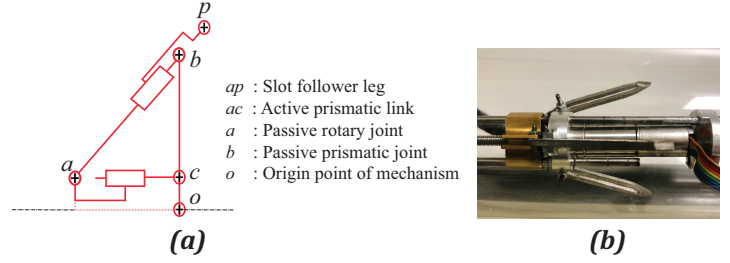


FIGURE 5: Representation of (a) the geometry of slot-follower leg mechanism and (b) the assembly of mechanism on the existing prototype [9, 10]

known. For simplifications, the optimization problem is solved by considering a two-dimensional projection of the geometry of two legs. This geometry of the leg mechanism that will be assembled on the robot is depicted in Fig. 6a. The design parameters for the leg mechanism (Fig. 6c) are the lengths l_{s1} , l_{s2} , the offsets o_1 , o_2 , the stroke lengths ρ_1 , ρ_2 and the horizontal and vertical space vectors $\Delta\mathbf{x}$ and $\Delta\mathbf{y}$ [9, 10]. The horizontal and vertical space vector of leg mechanism is given by $\Delta\mathbf{x} = [\Delta x_1, \Delta x_2]^T$ and $\Delta\mathbf{y} = [\Delta y_1, \Delta y_2]^T$. During locomotion of robot inside the pipeline, at least one set of leg mechanisms establish contact with pipeline walls. However, this sequence will be time-consuming to construct in MATLAB. In order to have faster convergence and a simpler model, it is assumed that at all positions of CLR both the set of leg mechanisms remain in the declamped phase during simulation. The design variables for the optimization problem is given by $[\Delta x_1, \Delta y_1, l_{s2}]$. The offsets o_1 and o_2 are retained as 11 mm and 7 mm, based on the existing prototype as these correspond to offsets caused by the EC-Motor unit (o_1) and spacers (o_2) used for assembly of leg mechanisms. The parameter Δx_1 is referenced from the frame Σ_0 using x_{m3} for Module-3 and x_{m1} for Module-1 as depicted in Fig. 6a.

Objective function

Since no leg masses are attached to the central motor, this module will not be taken into account for the second optimization problem. The objective function aims to maximize the space occupied by the leg mechanisms. This space can be split into triangular and rectangular area as represented in Fig. 6b. The area of the leg mechanisms used in the robot at a given discretized CLR point can be calculated by

$$f_2 = \sum_{k=1}^2 \left(\frac{\|\mathbf{e}_{k1}\mathbf{e}_{k2}\| \|\mathbf{e}_{k3}\mathbf{e}_{k2}\|}{2} + \frac{\|\mathbf{f}_{k1}\mathbf{f}_{k2}\| \|\mathbf{f}_{k3}\mathbf{f}_{k2}\|}{2} + \|\mathbf{e}_{k1}\mathbf{e}_{k3}\| \|\mathbf{e}_{k1}\mathbf{f}_{k1}\| \right) \quad (7)$$

where $i = 1, 2$ indicates Module-1 and Module-3

TABLE 3: MAXON CATALOG PARTS IDENTIFICATION WITH RESPECT TO RESULTS OF OPTIMIZATION FOR 100 TO 160 mm DIAMETER PIPES

Type	Series	Gear ratio	Feed force (N)	Efficiency (%)	Length (Motor+Spindle) (mm)
Motor	283828	5.4:1	189	87	46.4
Spindle	424731				
Motor	283828	29:1	331	79	51.5
Spindle	424744				
Motor	283828	455:1	403	69	58.7
Spindle	424749				

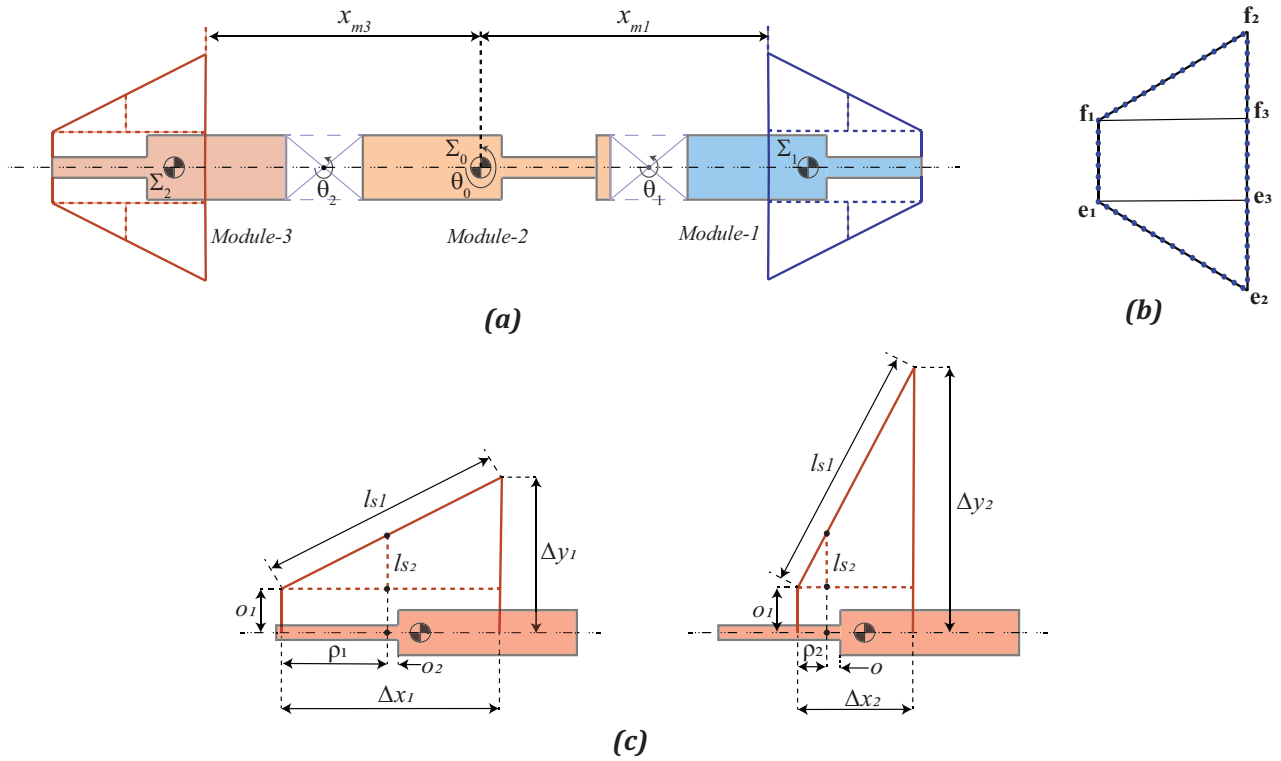


FIGURE 6: Representation of (a) the slot-follower leg mechanism on the robot, (b) the discretization of leg mechanism and (c) the design parameters defining the geometry of leg mechanism during declamping and clamping phases

Similar to Eqn. (4), the global sum of f_2 for Eqn. (7) is estimated which will be maximized.

Constraint function

At all positions of CLR, the collision of the geometry of leg mechanisms is verified against the pipeline walls. Inequality

constraints from Algorithm 2 are carried over to this optimization problem which will ensure that the discretized geometry of the leg mechanism avoids collisions with inner and outer portions of the pipe. However, the inequality constraints are reduced from 6 to 4 for this problem as the central module is not taken into account. The inequality constraint equations are similar to Eqn. (5)

& Eqn. (6) but instead, they apply only to the front and rear modules. Two additional equality constraints will be defined for this optimization problem. As the simulation is performed for fully declamped phases, the length of leg mechanism l_{s1} can be calculated from Fig. 6b using Pythagoras theorem and it is given by

$$l_{s1}(d) = \sqrt{\|\mathbf{f}_{k1}\mathbf{f}_{k3}\| + \|\mathbf{f}_{k2}\mathbf{f}_{k3}\|} \quad (8)$$

where $i = 1, 2$ indicates Module-1 and Module-3

In Eqn. (8), $l_{s1}(d)$ indicates the leg length during declamped phase. During the clamped phase, the length l_{s1} can be calculated with the help of Δx_2 , Δy_2 and o_1 by the Pythagoras theorem. Also during the declamped phase, the parameter l_{s2} can be estimated using similar triangles. The equations are given by

$$l_{s1}(c) = \sqrt{\Delta x_2^2 + (\Delta y_2 - o_1)^2} \quad (9)$$

$$\frac{l_{s2}}{\rho_1} = \frac{\Delta y_1 - o_1}{\Delta x_1} \quad (10)$$

In Eqn. (9), $l_{s1}(c)$ is the length of the leg mechanism during clamped phase. The stroke lengths ρ_1 and ρ_2 are set as 32 mm and 7 mm with reference to the 45 mm screw length of motor unit for 100 mm diameter pipe (Table 2). The reduction in stroke length is caused by flanges and fasteners that will be used for the robot assembly. The two equality constraints for the second optimization problem are thus given by

$$h_1 : \rho_1 = 32 \quad (11)$$

$$h_2 : l_{s1}(d) = l_{s1}(c) \quad (12)$$

Problem statement

For the second optimization problem, the diameter d of the pipeline is fixed as 100 mm. The optimization problem to estimate the size of the leg mechanisms can be defined by

$$\text{maximize } \sum_{i=1}^n f_2(\mathbf{z})$$

subject to constraints: $g_1, g_2, g_3, g_4, h_1, h_2$

$$\text{where } \mathbf{z} = [\Delta x_1, \Delta y_1, l_{s2}]^T,$$

$i = 1..n$ indicates the discretized CLR positions

The lower and upper bounds of the design parameters for the simulation are given by $lb = [40, 20, 5]$, $ub = [65, 40, 12]$. In

Eqn. (9), the value of Δy_2 is fixed as 60% of the pipe diameter taken for simulation. A value higher than 60% leads to convergence issues for a screw length of 45 mm. With the limit of ρ_2 set to 7 mm, the value of Δx_2 can be calculated using similar triangles. Using the *fmincon* function with the SQP algorithm, the optimization problem is solved to determine the geometry of leg mechanisms.

Results and discussions

The dimensions of the slot-follower leg mechanism after optimization are provided below in Table 4.

TABLE 4: RESULTS OF OPTIMIZATION PROBLEM-2: SLOT-FOLLOWER DIMENSIONS

Parameters	Dimensions (mm)
Δx_1	60
Δy_1	29.3
Δy_2	62
l_{s1}	62.7
l_{s2}	9.7

Compared to the existing prototype, the parameters l_{s1} and l_{s2} are increased from 57 mm and 7 mm to 62.7 mm and 9.7 mm respectively. In the event of a straight pipeline with no bends, the slot-follower leg mechanism is capable of adjusting its size between 58.6 mm ($2\Delta y_1$) to 124 mm ($2\Delta y_2$) diameter range. When the robot is moving inside a pipeline with bends, the modules are capable of passing through such bends provided the diameter of pipelines is strictly between 100 to 120 mm. By assembling the tensegrity mechanism, the EC-motor with spindle drive unit identified from optimization problem-1, the optimized slot-follower leg mechanism and standard fasteners such as circlips, bolts etc., the entire robot can be realized using CATIA software. The locomotion of the robot inside a 100 mm diameter is rendered using CATIA and the sequence is represented in Fig. 7a to Fig. 7e. The reconfigurable robot resembles an ‘‘Elephant trunk’’ and it is demonstrated in Fig. 7f.

CONCLUSIONS

In this article, an optimization approach was employed to determine the sizing of the robot and its associated leg mechanism to pass through pipe bends. Two problems were defined and

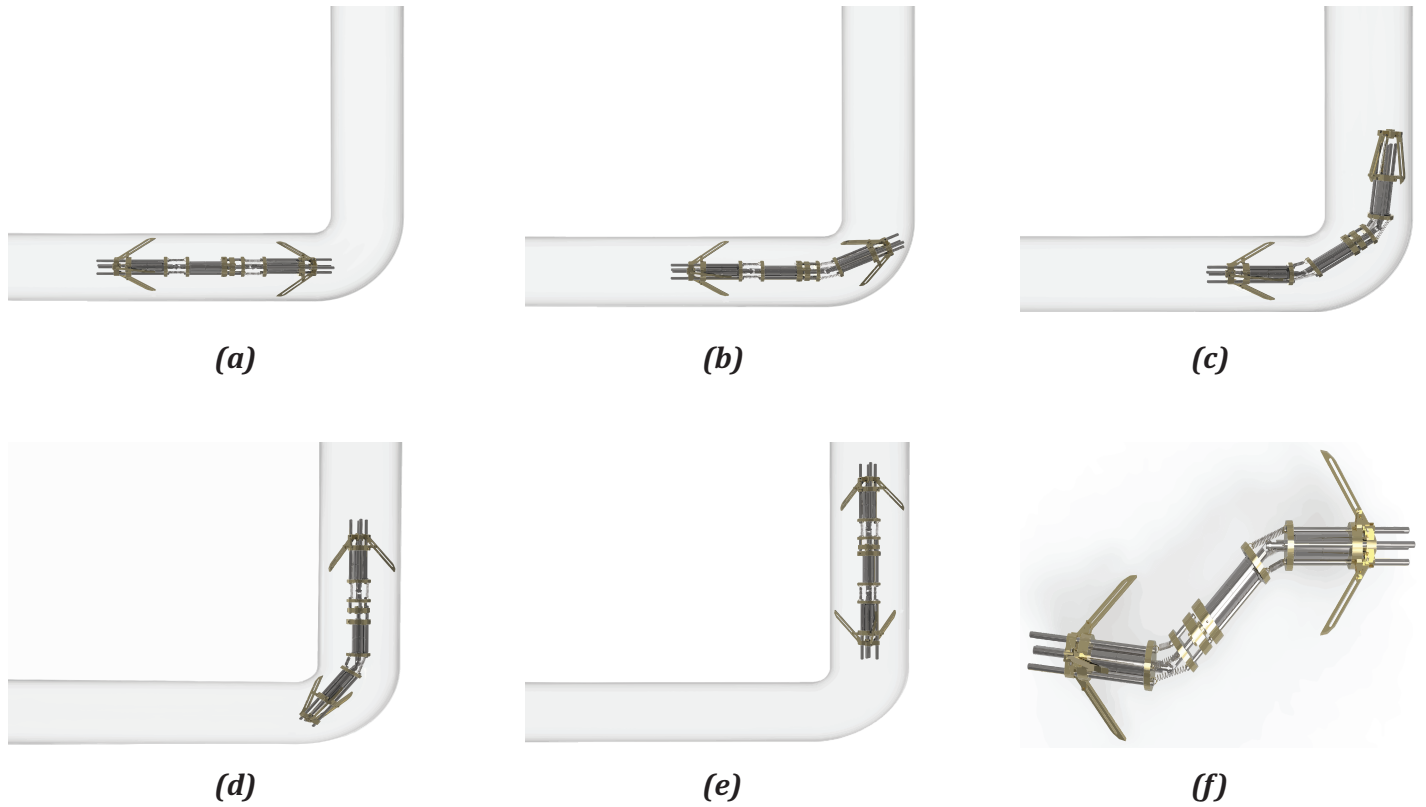


FIGURE 7: Locomotion sequence of the optimized bio-inspired robot inside a 100 mm diameter pipe from (a) to (e) and correlation of the robot to an “Elephant trunk” (f)

solved in this article which employed the deterministic optimization approach in MATLAB. The first problem dealt with the estimation of sizes of individual motor modules without the presence of leg mechanisms inside a test bench with different diameters. From the results of optimization, the dimensions for 100 mm diameter pipe were chosen to have a nominal screw length that can accommodate the slot-follower leg mechanism for the second problem. The catalog parts of Maxon were identified based on the results of the first optimization problem. Followed by that, in the second problem the sizing of the slot-follower leg mechanism was determined by a geometric approach that did not require the kinematic models. The dimensions of the slot-follower leg mechanism were found to be increased when compared to the existing prototype. However, with the modified architecture, the robot is capable of working inside 100–120 mm diameter pipeline range that can have straight sections and bends at 90° . The presence of leg mechanisms and tensegrity mechanism permits to have a reconfigurable “Elephant trunk” model that allows the robot to pass through pipe bends.

In future works, the optimization algorithm can be modified to accommodate a relation between screw length and pipeline diameter thereby reducing user efforts to fix the pipeline diameters

for each computation. This modification might probably lead to the definition of another objective and evolutionary algorithms will be implemented to solve this problem. With the 3D model being assembled using catalog parts, the static force model developed in [9] can be extended to the reconfigurable robot. This model can help in determining the forces on the tensegrity mechanisms as well as the maximum clamping forces which can be useful for performing experiments. A simulation of the robot will be performed using ADAMS software to validate the locomotion procedure followed by which prototyping of the reconfigurable robot will be done. For the real-time application, suitable control units and a camera will be accommodated on the robot to perform an inspection of pipelines.

REFERENCES

- [1] Choi, H. R., and Roh, S.-g., 2007. “In-pipe robot with active steering capability for moving inside of pipelines”. In *Bioinspiration and Robotics Walking and Climbing Robots*. IntechOpen.
- [2] Okamoto Jr, J., Adamowski, J. C., Tsuzuki, M. S., Buiocchi, F., and Camerini, C. S., 1999. “Autonomous system for oil

- pipelines inspection”. *Mechatronics*, **9**(7), pp. 731–743.
- [3] Okada, T., and Kanade, T., 1987. “A three-wheeled self-adjusting vehicle in a pipe, ferret-1”. *The International journal of robotics research*, **6**(4), pp. 60–75.
- [4] Roman, H. T., Pellegrino, B., and Sigrist, W., 1993. “Pipe crawling inspection robots: an overview”. *IEEE transactions on energy conversion*, **8**(3), pp. 576–583.
- [5] Ryew, S., Baik, S., Ryu, S., Jung, K. M., Roh, S., and Choi, H. R., 2000. “In-pipe inspection robot system with active steering mechanism”. In Proceedings. 2000 IEEE/RSJ International Conference on Intelligent Robots and Systems (IROS 2000)(Cat. No. 00CH37113), Vol. 3, IEEE, pp. 1652–1657.
- [6] Neubauer, W., 1994. “A spider-like robot that climbs vertically in ducts or pipes”. In Proceedings of IEEE/RSJ International Conference on Intelligent Robots and Systems (IROS’94), Vol. 2, IEEE, pp. 1178–1185.
- [7] Fukuda, T., Hosokai, H., and Uemura, M., 1989. “Rubber gas actuator driven by hydrogen storage alloy for in-pipe inspection mobile robot with flexible structure”. In Proceedings, 1989 international conference on robotics and automation, IEEE, pp. 1847–1852.
- [8] Horodincu, M., Doroftei, I., Mignon, E., and Preumont, A., 2002. “A simple architecture for in-pipe inspection robots”. In Proc. Int. Colloq. Mobile, Autonomous Systems, pp. 61–64.
- [9] Venkateswaran, S., Chablat, D., and Boyer, F., 2019. “Numerical and experimental validation of the prototype of a bio-inspired piping inspection robot”. *Robotics*, **8**(2), p. 32.
- [10] Henry, R., Chablat, D., Porez, M., Boyer, F., and Kanaan, D., 2014. “Multi-objective design optimization of the leg mechanism for a piping inspection robot”. In Proceedings of the ASME 2014 IDETC-CIE, Vol. 5A: 38th Mechanisms and Robotics Conference. V05AT08A001.
- [11] Chablat, D., Venkateswaran, S., and Boyer, F., 2019. “Dynamic model of a bio-inspired robot for piping inspection”. In *ROMANSY 22—Robot Design, Dynamics and Control*. Springer, pp. 42–51.
- [12] Venkateswaran, S., and Chablat, D., 2019. “A new inspection robot for pipelines with bends and junctions”. In IFToMM World Congress on Mechanism and Machine Science, Springer, pp. 33–42.
- [13] Guessasma, S., and Bassir, H., 2009. “Comparing heuristic and deterministic approaches to optimise mechanical parameters of biopolymer composite materials”. *Mechanics of Advanced Materials and Structures*, **16**(4), pp. 293–299.
- [14] Rao, R. V., and Waghmare, G., 2017. “A new optimization algorithm for solving complex constrained design optimization problems”. *Engineering Optimization*, **49**(1), pp. 60–83.
- [15] Venkateswaran, S., Furet, M., Chablat, D., and Wenger, P., 2019. “Design and analysis of a tensegrity mechanism for a bio-inspired robot”. In Proceedings of the ASME 2019 IDETC-CIE, Vol. 5A: 43rd Mechanisms and Robotics Conference. V05AT07A026.
- [16] Li, H., Yang, H., Zhan, M., and Gu, R., 2007. “The interactive effects of wrinkling and other defects in thin-walled tube nc bending process”. *Journal of Materials Processing Technology*, **187**, pp. 502–507.
- [17] Venkateswaran, S., Chablat, D., and Ramachandran, R., 2019. “Prototyping a piping inspection robot using a beaglebone black board”. In 24^{ème} Congrès Français de Mécanique, Brest.
- [18] Maxon Motors, Program 2017/18. High precision Drives and Systems. <http://epaper.maxonmotor.com/>. Accessed: 2019-12-15.
- [19] Choosing the algorithm- MATLAB & Simulink- Mathworks France. <https://fr.mathworks.com/help/optim/ug/choosing-the-algorithm.html>. Accessed: 2020-02-02.

NOMENCLATURE

Symbol	Description
CG	Center of gravity
CLR	Center line radius
\mathbf{o}	Reference point for test bench pipe
$\mathbf{a}_i, \mathbf{b}_i, \mathbf{c}_i, \mathbf{d}_i$	Coordinates of trajectory i of test bench
d	Diameter of pipe/test bench
Σ_0	Reference frame for robot at Module-2
Σ_1, Σ_2	Frames of Module-1 & Module-3
$\theta_0, \theta_1, \theta_2$	Rotation angles of Module 1,2 & 3
l_1	Length of motor unit (EC motor+Spindle drive)
w_1	Width/diameter of motor unit (EC motor+Spindle drive)
l_2	Length of screw of spindle drive
w_2	Width/diameter of screw of spindle drive
f_1, f_2	Objective function variable for problem-1 & problem-2
g	Inequality constraint equation variable
h	Equality constraint equation variable
lb, ub	Lower and upper bounds for design variables
l_{s1}	Length of slot-follower leg mechanism
l_{s2}	Design parameter of leg mechanism
$\Delta x_1, \Delta x_2$	Horizontal space occupied by leg during declamping & clamping
$\Delta y_1, \Delta y_2$	Vertical space occupied by leg during declamping & clamping
ρ_1, ρ_2	Leg stroke lengths during declamping & clamping